MADRID
inter.noise 2019
June 16 - 19
NOISE CONTROL FOR A BETTER ENVIRONMENT

Reducing acoustic loads on a spacecraft inside a rocket fairing

Igolkin, Aleksandr[1]
Samara National Research University named S.P. Korolev
443086 Samara, ul. Moskovskoe shosse Street 34

Popov, Pavel[2]
Samara National Research University named S.P. Korolev
443086 Samara, ul. Moskovskoe shosse Street 34

Shakhmatov, Evgeniy[3]
Samara National Research University named S.P. Korolev
443086 Samara, ul. Moskovskoe shosse Street 34

ABSTRACT

Reducing acoustic loads on complex shape objects placed inside a cylindrical shell result in design challenges. An example of such a task is accommodation of the spacecraft (SC) inside the fairing of a launch vehicle. The paper presents a mathematical model for determining acoustic loads acting on the spacecraft depending on the acoustic absorption factor of the fairing surface, SC and the SC configuration. As a result, we have received spectra of root-mean-square acoustic pressure levels which make it possible to adapt this SC to the requirements of the fairing.

Keywords: fairing, spacecraft configuration, acoustic power, sound intensity
I-INCE Classification of Subject Number:32

1.INTRODUCTION

Cases emerge when a ready designed spacecraft, previously deployed by another launch vehicle (LV), has to be adapted to the fairing of the Soyuz rocket. If this new LV acoustic loads are acting in the existing spacecraft to which it has not been designed and developed, then it is necessary to develop measures to reduce them. In the present work, the problem of a scientifically justified selection of the fairing characteristics for satisfying the acoustic loading parameters specified for the SC is solved, with its adaptation to the standard requirements of the Soyuz type LV (Fig. 1a).

On the basis of [1,2,3], we have generated acoustic loading modes on the surface of a spacecraft when it filled the fairing section up to 50%.

[1] igolkin97@gmail.com
[2] banduir@rambler.ru
[3] shakhm@ssau.ru

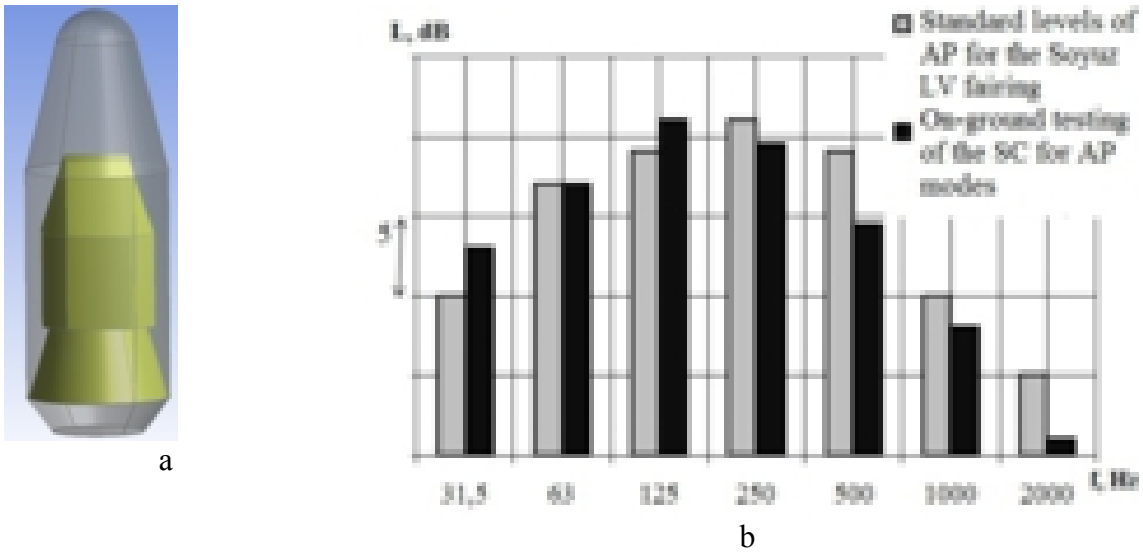

a b

Fig. 1. "Soyuz" LV fairing design with a SC (a), frequency distributions of AP levels for the fairing and SC (b).

In Fig. 1b we have shown the frequency distribution of the acoustic pressure levels for which an adaptive SC and the acoustic pressure levels for the fairing generated under the condition of 10% absorption of acoustic energy by the SC design, α_{SC} =0.1 [1]. An analysis of Fig. 1b demonstrates that at frequencies of 250 Hz -2000 Hz, the acoustic pressure under the existing fairing is noticeably higher than the corresponding values for the adaptive space vehicle. Therefore, it is necessary to choose such design parameters of sound-absorbing materials that the acoustic pressure levels do not exceed the design parameters of the adaptive spacecraft.

The task of reducing acoustic pressure in the aircraft compartments including LV and fairings was carried out by special task research groups at TsAGI. The results of these studies contain extensive information on the characteristics of shells and soundproof materials for compartments, such as sound insulation, sound absorption ratios, mechanical losses, permanent damping, and propagation constants [1,4,5,6,7,8,9,10,11,12]. However, in the research papers listed above, there is no data on the effect of the shape of the SC under the fairing and the acoustic absorption coefficient of the corresponding surfaces. Therefore, there was a need to develop a mathematical model for calculating the level of acoustic pressure, taking into account the shape and absorption by surfaces in the case of the spacecraft and fairing.

2. MATHEMATICAL MODEL

Let us first consider the simplest case when the "fairing-SC" system is represented in the form of two cylindrical surfaces (Fig. 2).

The outer cylinder is the fairing shell, the inner cylinder imitates the SC. Let the surface of the fairing emit an acoustic field of power *N*, W into the interior space, then the intensity of the field at the point on the surface of the fairing:

$$J = \frac{N}{2\pi RH}. \tag{1}$$

The acoustic power emitted by the surface element *ds* from (1) is represented in the form:

$$dN_1 = \frac{N}{2\pi RH} ds = \frac{N}{2\pi RH} Rd\varphi dz. \tag{2}$$

The flow of acoustic energy propagating through *ds* (Fig. 3b) has passed the *SS′* path while it has been dispersed in accordance with the law [13,14]:

$$|SS'|^2 = R^2 + r^2 - 2Rr\cos(\varphi) + z^2 .$$

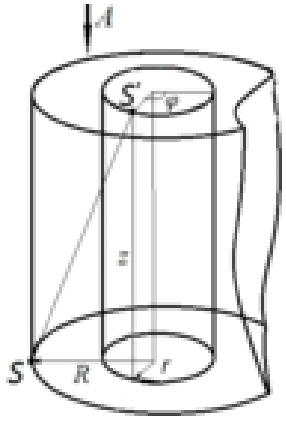

a

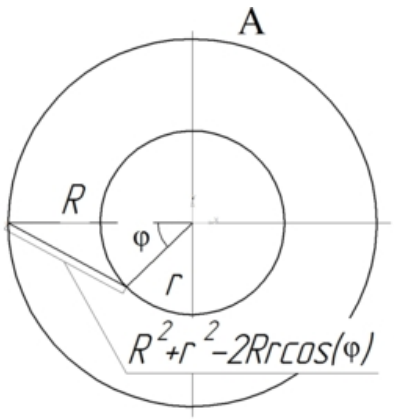

b

Fig.2. Fairing-SC system in the form of cylindrical surfaces (a), top view of the Fairing-SC system (b): *R* - radius of the fairing, *r*- radius of the spacecraft, *z,* φ- longitudinal coordinate and polar angle over which integration is carried out.

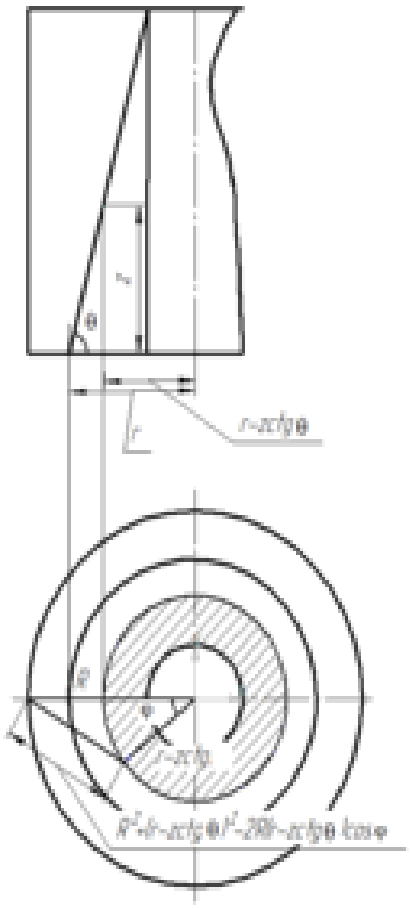

Fig. 3. Fairing-SC system of a conical configuration: *R* - radius of the fairing, *r* - radius of the base of the conical spacecraft, *z* - variable of integration along the height, *φ* - angle of integration.

The sound intensity on the SC surface became equal to:

$$I_1^{SC} = \int_0^{H_{SC}} \int_{-\arccos(r/R)}^{\arccos(r/R)} \frac{N}{2\pi RH\Omega\,|SS'|^2} Rd\varphi dz \qquad (3)$$

After being reflected from the SC surface, part of the energy was absorbed by its structure and the sound intensity became equal to:

$$I_1^{SC} = \int_0^{H_{SC}} \int_{-\arccos(r/R)}^{\arccos(r/R)} \frac{N(1-\alpha_{SC})}{2\pi RH\Omega\,|SS'|^2} Rd\varphi dz. \qquad (4)$$

After that, the flow of acoustic energy returned to the fairing:

$$I_1^{\ F} = \int_0^{H_{SC}} \int_{-\arccos(r/R)}^{\arccos(r/R)} \frac{N(1-\alpha_{SC})}{2\pi RH\Omega 2\,|SS^{'}|^2} Rd\varphi dz.$$

And reflected from the surface of the fairing:

$$I_2 = \int_0^{H_{SC}} \int_{-\arccos(r/R)}^{\arccos(r/R)} \frac{N(1-\alpha_{SC})(1-\alpha_F)}{2\pi RH\Omega 2\,|SS^{'}|^2} Rd\varphi dz,$$

where α_F – absorption ratio by the fairing structure.

We are interested only in those terms of the forms (3) and (4) that characterize the SC acoustic loading, therefore, by continuing this process an infinite number of times for the total sound intensity, we will obtain:

$$I_{SC}^{\Sigma} = \sum_{i=1}^{\infty} \int_0^{H_{SC}} \int_{-\arccos(r/R)}^{\arccos(r/R)} \left(\frac{N(1-\alpha_{SC})^{i-1}(1-\alpha_F)^{i-1}}{(2\pi)^2 RH(2i-1)(R^2+r^2-2Rr\cos(\varphi)+z^2)} + \right.$$
$$\left. + \frac{N(1-\alpha_{SC})^{i}(1-\alpha_F)^{i-1}}{(2\pi)^2 RH(2i-1)(R^2+r^2-2Rr\cos(\varphi)+z^2)}\right) Rd\varphi dz. \qquad (5)$$

For the case of a conic surface, arguing in a similar way, we will obtain the corresponding relations while taking into account the angle between the generatrix and the SC base, α (construction geometry is shown in Figure 3).

$$\begin{cases} dN_1 = \dfrac{N}{2\pi RH} Rd\varphi dz, \\ I_1^{SC} = \displaystyle\int_0^{H_{SC}} \int_{-\arccos((r\ -zctg(\alpha))/R)}^{\arccos((r\ -zctg(\alpha))/R)} \frac{NRd\varphi dz}{2\pi RH(R^2+(r-zctg(\alpha))^2-2R(r-zctg(\alpha))\cos(\varphi)+z^2)}, \\ I_1^{SC_{ref}} = \displaystyle\int_0^{H_{SC}} \int_{-\arccos((r\ -zctg(\alpha))/R)}^{\arccos((r\ -zctg(\alpha))/R)} \frac{N(1-\alpha_{SC})Rd\varphi dz}{2\pi RH(R^2+(r-zctg(\alpha))^2-2R(r-zctg(\alpha))\cos(\varphi)+z^2)}, \\ I_1^{F} = \displaystyle\int_0^{H_{SC}} \int_{-\arccos((r\ -zctg(\alpha))/R)}^{\arccos((r\ -zctg(\alpha))/R)} \frac{N(1-\alpha_{SC})Rd\varphi dz}{2\pi RH2(R^2+(r-zctg(\alpha))^2-2R(r-zctg(\alpha))\cos(\varphi)+z^2)}, \end{cases}$$

$$\begin{cases} I_2^{SC} = \displaystyle\int_0^{H_{SC}} \int_{-\arccos((r\ -zctg(\alpha))/R)}^{\arccos((r\ -zctg(\alpha))/R)} \frac{N(1-\alpha_{SC})(1-\alpha_F)Rd\varphi dz}{2\pi RH2(R^2+(r-zctg(\alpha))^2-2R(r-zctg(\alpha))\cos(\varphi)+z^2)}, \\ I_2^{SC_{ref}} = \displaystyle\int_0^{H_{SC}} \int_{-\arccos((r\ -zctg(\alpha))/R)}^{\arccos((r\ -zctg(\alpha))/R)} \frac{N(1-\alpha_{SC})(1-\alpha_F)Rd\varphi dz}{2\pi RH3(R^2+(r-zctg(\alpha))^2-2R(r-zctg(\alpha))\cos(\varphi)+z^2)}, \\ I_2^{F} = \displaystyle\int_0^{H_{SC}} \int_{-\arccos((r\ -zctg(\alpha))/R)}^{\arccos((r\ -zctg(\alpha))/R)} \frac{N(1-\alpha_{SC})^2(1-\alpha_F)Rd\varphi dz}{2\pi RH3(R^2+(r-zctg(\alpha))^2-2R(r-zctg(\alpha))\cos(\varphi)+z^2)}, \\ I_2^{F_{ref}} = \displaystyle\int_0^{H_{SC}} \int_{-\arccos((r\ -zctg(\alpha))/R)}^{\arccos((r\ -zctg(\alpha))/R)} \frac{N(1-\alpha_{SC})^2(1-\alpha_F)Rd\varphi dz}{2\pi RH4(R^2+(r-zctg(\alpha))^2-2R(r-zctg(\alpha))\cos(\varphi)+z^2)}. \end{cases}$$

For the *i* drop-reflection process for the SC conic space under study, we have:

$$I_i^{SC} = \int_0^{H_{SC}} \int_{-\arccos((r-zctg(\alpha))/R)}^{\arccos((r-zctg(\alpha))/R)} \frac{N(1-\alpha_{SC})^{i-1}(1-\alpha_F)^{i-1} Rd\varphi dz}{2\pi RH(2i-1)(R^2+(r-zctg(\alpha))^2-2R(r-zctg(\alpha))\cos(\varphi)+z^2)},$$

$$I_i^{SC_{ref}} = \int_0^{H_{SC}} \int_{-\arccos((r-zctg(\alpha))/R)}^{\arccos((r-zctg(\alpha))/R)} \frac{N(1-\alpha_{SC})^{i}(1-\alpha_F)^{i-1} Rd\varphi dz}{2\pi RH(2i-1)(R^2+(r-zctg(\alpha))^2-2R(r-zctg(\alpha))\cos(\varphi)+z^2)}.$$

The total level of the falling and reflected values of the sound intensity:

$$I_{SC}^{\Sigma} = \sum_{i=1}^{\infty} \int_0^{H_{SC}} \int_{-\arccos((r-zctg(\alpha))/R)}^{\arccos((r-zctg(\alpha))/R)} \left(\frac{N(1-\alpha_{SC})^{i-1}(1-\alpha_F)^{i-1}}{\begin{cases} 2\pi RH(2i-1)(R^2+(r-zctg(\alpha))^2- \\ -2R(r-zctg(\alpha))\cos(\varphi)+z^2) \end{cases}} + \right. \tag{6}$$

$$\left. + \frac{N(1-\alpha_{SC})^{i}(1-\alpha_F)^{i-1}}{\begin{cases} 2\pi RH(2i-1)(R^2+(r-zctg(\alpha))^2- \\ -2R(r-zctg(\alpha))\cos(\varphi)+z^2) \end{cases}} \right) Rd\varphi dz.$$

For the case of a truncated pyramidal surface that has a rectangle or a square at its base, a formula similar to expressions (5), (6) expressing the result of simulating will take the form:

$$I^{\Sigma} = \sum_{i=1}^{\infty} \int_0^{H_{SC}} \int_{-\operatorname{arctg}\left(\frac{\frac{a_2}{2}-zctg(\theta)}{\frac{a_1}{2}-zctg(\theta)}\right)}^{\operatorname{arctg}\left(\frac{\frac{a_2}{2}-zctg(\theta)}{\frac{a_1}{2}-zctg(\theta)}\right)} \left(\frac{N(1-\alpha_{SC})^{i-1}(1-\alpha_F)^{i-1}}{\begin{cases} (2\pi)^2 RH(2i-1)(((\frac{a_1}{2}-zctg(\theta))tg(\varphi)-R\sin(\psi))^2+ \\ +(R\cos(\psi)-\frac{a_1}{2}+zctg(\theta))^2+z^2) \end{cases}} + \right.$$

$$\left. + \frac{N(1-\alpha_{SC})^{i}(1-\alpha_F)^{i-1}}{\begin{cases} (2\pi)^2 RH(2i-1)(((\frac{a_1}{2}-zctg(\theta))tg(\varphi)-R\sin(\psi))^2+ \\ +(R\cos(\psi)-\frac{a_1}{2}+zctg(\theta))^2+z^2) \end{cases}} \right) Rd\varphi dz. \tag{7}$$

where H_{SC}, r, α_{SC} – SC height, radius, surface absorption ratio; R, α_F – radius and absorption ratio of the fairing, N – power of the acoustic pressure transmitted through the fairing structure, φ – angle of integration sliding on the SC base and fairing, z – integration by the SC height, a_1, a_2 – The sides of the rectangle at the base of the cone (in our case later $a_1=a_2$, therefore the limits of integration will be φ=-π/4..+π/4- angle sliding over the rectangular side of the SC, ψ=-π/4..+ π/4 – angle sliding over the cylinder of the fairing, θ – angle between the base and the generatrix of the pyramid.

For the case of a rectangular section of the spacecraft, formula (8) takes a simpler form:

$$N^{\Sigma}=\sum_{i=1}^{\infty}\int_{0}^{H_{SC}}\int_{-\frac{\pi}{4}}^{\frac{\pi}{4}}\left(\frac{N(1-\alpha_{SC})^{i-1}(1-\alpha_{F})^{i-1}}{\left\{\begin{array}{l}(2\pi)^2 RH(2i-1)((\frac{a_1}{2}tg(\varphi)-R\sin(\psi))^2+\\ +(R\cos(\psi)-\frac{a_1}{2})^2+z^2)\end{array}\right.}+\frac{N(1-\alpha_{SC})^{i}(1-\alpha_{F})^{i-1}}{\left\{\begin{array}{l}(2\pi)^2 RH(2i-1)((\frac{a_1}{2}tg(\varphi)-R\sin(\psi))^2+\\ +(R\cos(\psi)-\frac{a_1}{2})^2+z^2)\end{array}\right.}\right)Rd\varphi dz. \quad (8)$$

Formulas (5) - (8) are the result of modeling the processes of incidence and reflection of acoustic energy inside the fairing onto the SC in the form of a cylinder, a truncated cone, a pyramid or a parallelogram. Depending on the closeness of the geometry of a real spacecraft, one or another mathematical model is chosen.

The selected model uses the actual absorption ratio of the SC surface $\alpha_{SC}=\alpha_{SC}(f)$ (it was previously noted that for the calculation of specification levels $\alpha_{SC}=0.1$ was used within the whole operational spectrum of frequencies).

If the calculation for the selected model showed that the reduced acoustic pressure meets the requirements of the technical documentation of the spacecraft, then this acoustic pressure is input into the design documentation for the item adapted to the fairing, otherwise, it is necessary to increase the absorption ratios α_{SC}, α_F by placing on the SC or fairing surface some other materials with increased values of absorption in critical frequency bands.

3. SAMPLE CALCULATIONS

As an example, let us consider the spacecraft developed earlier for LV producing lower noise levels. This SC was tested for spectral levels of acoustic pressure is shown in Fig. 1b (black line).

As can be seen from Fig. 1a, SC represents squares with beveled corners, with the upper part of the SC close in shape to a truncated pyramid, the lower part - to a cube. The sound intensity for a given spacecraft was first calculated for the case $\alpha=0.1$ within the entire frequency range according to formulas (8), (9) for the upper and lower parts of the spacecraft, respectively. A comparative analysis of the spectra in Fig. 1b shows that in octave bands from 250 Hz to 2000 Hz, there are exceedances that do not allow to meet the requirements of the technical specification for this particular spacecraft. To sufficiently reduce the levels of acoustic loading in high-frequency bands, it has been proposed:

1) Apply a PU foam as a sound-absorbing material with an increased thickness from 20 mm to 50 mm which according to the calculation [4] will improve the characteristics of the acoustic field in accordance with Table 1.

Table 1. Reduction of acoustic pressure at increasing the thickness of the PU foam-35 layer from 20 mm to 50 mm

Frequency, *Hz*	125	250	500	1000	2000
Reduction of AP, *dB, (ΔL_1)*	0,2	0,9	3,2	4,2	4,3

This measure allows to implement sufficient reduction of acoustic pressure in octave bands from 1000 Hz to 2000 Hz.

2) To further reduce the acoustic pressure, it is recommended for the developer of the spacecraft to install electro-vacuum thermal insulation mats on the side surface of the spacecraft. With the help of the mathematical model described above, by formulas (8) and (9) we calculated the reduction of the sound intensity levels ΔL_2 for the fairing when using the electro-vacuum thermal insulation material on the spacecraft and under the condition of applying the PU foam in the fairing:

$$\Delta L_2 = 10\lg(\frac{I_1}{I_2}),\ L = L_n - \Delta L,$$

where I_1, I_2 – the sound intensity for the fairing before and after the implemented measures, respectively, L_n, L - the initial (normal) and the reduced level under the fairing. The normal absorption coefficient for electro-vacuum thermal insulation material and PU foam was taken from [4,16].

In addition to the calculations by formulas (8) and (9), an analysis was made of the acoustic loading reduction according to the known formula [13, 17] which does not take into account the shape of the fairing and SC:

$$\Delta L_2 = 10\lg(\frac{\sum_{i=1}^{n} S_i \alpha_i}{\sum_{i=1}^{n} S_i}),$$

where S_i – surface area of the fairing and SC, α_i – corresponding to the specific S_i acoustic energy absorption.

The results of the calculations are shown in Fig.4.

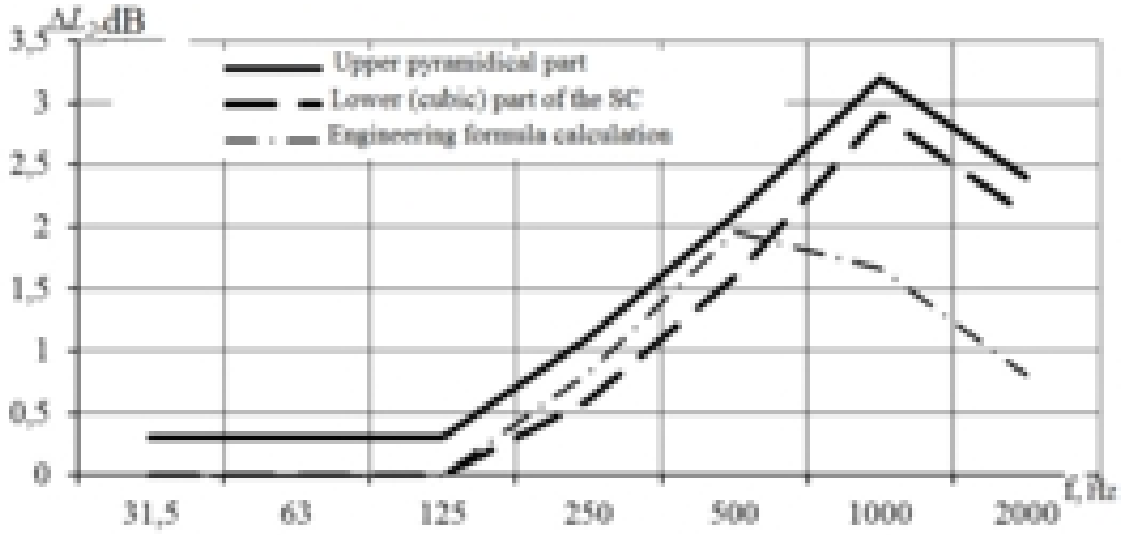

Fig. 4. The results of calculations by formulas (8), (9) and the engineering formula [13, 17] showing the drop in acoustic loading when the electro-vacuum thermal insulation material is applied.

The values of the total reduction in the sound intensity levels (or the root-mean-square acoustic pressure level [13]) on the SC are presented in Table 2.

Table 2. The total decrease in the levels of sound intensity (or the mean square acoustic pressure level) acting on the SC

Frequency, *Hz*	250	500	1000	2000
Reduction of the AP levels on the SC lower part, *dB*	1,4	4,3	6,1	5,6
Reduction of the AP levels on the SC upper part, *dB*	1,9	4,7	6,3	5,8

A similar analysis was carried out in [16], where the results for a generalized spacecraft (without a definite shape) were presented in Fig. 5.

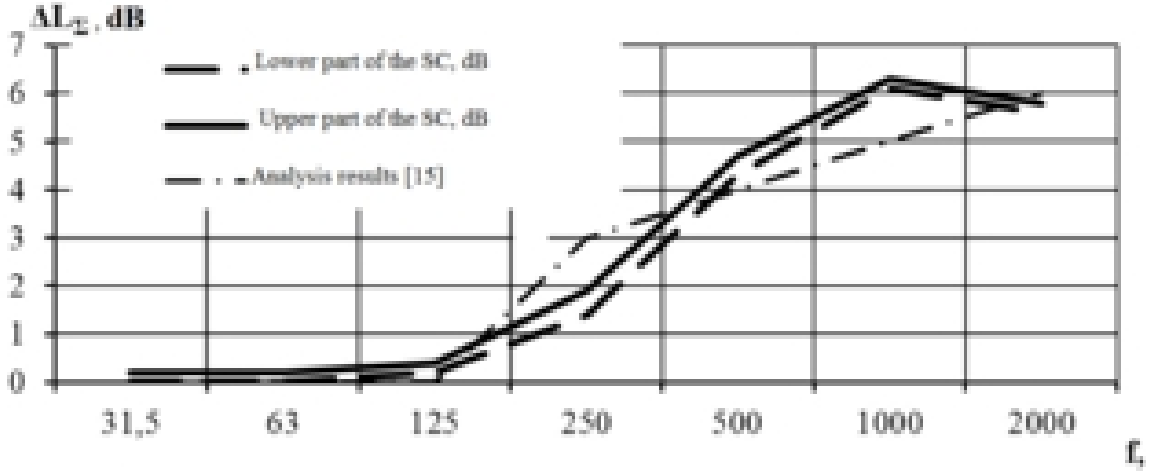

Fig. 5. Calculated total decrease in the levels of acoustic pressure acting on the SC and the result presented in [15] for a SC generalized by shape.

Subtracting the values of Table 2 from the standard levels, the distributions of which are shown in Fig. 1b, we obtain the following distributions, shown in Fig.6.

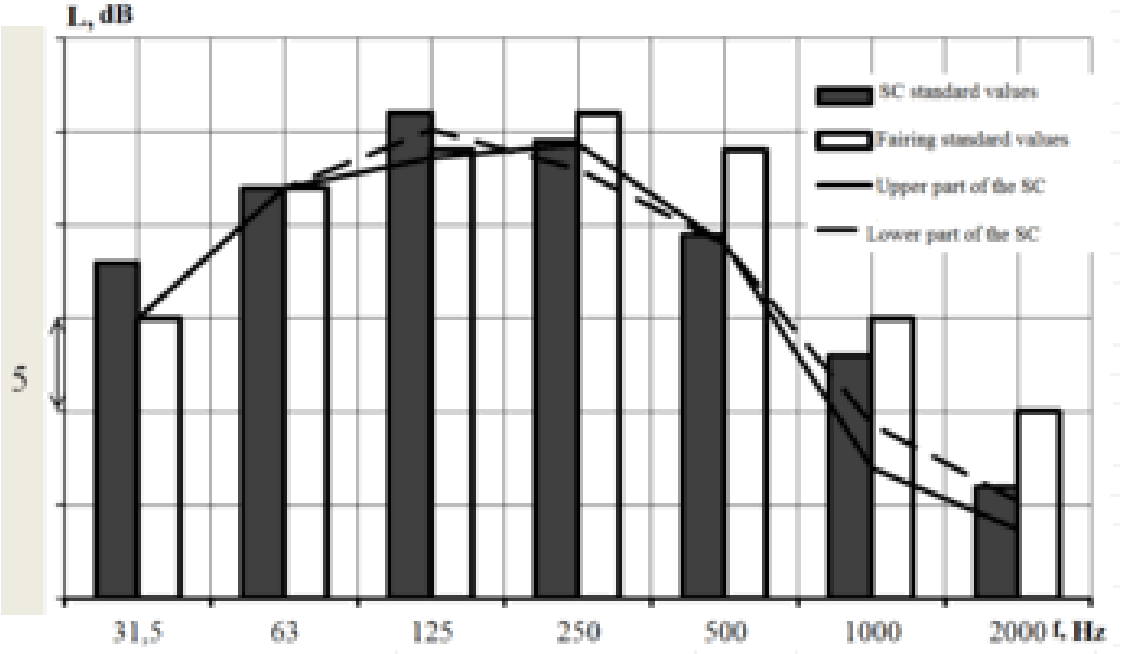

Fig. 6. Frequency distributions of AP levels during the SC ground testing and the AP levels of the lower and upper parts of the SC in operation.

From considering Fig. 6 we deduce that due to the additional absorption of acoustic energy by the electro-vacuum thermal insulation material and the thickened material of the PU foam, a reduction in the initial levels of mean square AP was achieved. The newly obtained RMS levels did not exceed the values for which the adaptive spacecraft was tested.

4. CONCLUSIONS

Within the framework of the work performed, the following results have been obtained:

1. A refined mathematical model has been developed to evaluate the effect of the shape of the spacecraft and absorption factors on the acoustic field acting on the SC in its various structural parts.
2. Calculation estimation has been made in accordance with which, in order to fulfill the requirements of the technical assignment, constructive measures were taken to reduce the acoustic pressure levels.

The mathematical model used in this research paper can be used later to estimate the intensity of sound acting on the spacecraft of other configurations (a cylinder, a cone, a sphere, etc.).

Further development of the research will allow selecting the area of application of soundproof materials to reduce acoustic loads to the required levels with allowable weight gain.

5. ACKNOWLEDGEMENTS

The authors would like to express their gratitude to the Russian Ministry of Education and Science for the financial support of the investigations (Project #9.1517.2017/PCh – 9.1517.2017/4.6).

6. REFERENCES

1. Calculated estimation of sound insulation and acoustic pressure spectra under the fairing at launch and flight of the Soyuz-2 launch vehicle / NTO, №4/11-03, RUSAVIA, 2003. 51 p.
2. The main results of vibroacoustic measurements of LV and the fairing at flight tests of LV 14A14-1a No. 3L/NTO, TsSKB, 2007. 309 p.
3. The main results of vibroacoustic measurements on LV and the fairing at flight tests of LV 14A14-1b with "Meteor-M" spacecraft/TsSKB, 2009. 370 p.
4. Calculation-experimental determination of acoustic loads for a metal fairing/NTO, No.5548, TsAGI, 1999. 71 p.
5. Determination of vibroacoustic characteristics of structural parts of the Soyuz LV fairing/NTO № 5527, TsAGI, 1999.43 p.
6. B.M. Efimtzov, L.A. Lazarev. Analysis of the sound-insulating capacity of resonant systems panels based on equivalent representations// Acoustic journal. 2005. Volume 51, №3. 360-365.
7. B.M. Efimtzov, A.Ya. Zverev. Acoustic field in a shell from two synchrophased sources // Acoustic journal. 1992. Volume 38, pages 693-701.
8. L.Ya. Kudisova, B.D. Tartakovsky. Propagation of sound through a reinforced plate // Acoustic journal. 1974. Volume 20, No. 1. Pages 55-61.
9. IVBelyaev, A.Yu.Golubev, A.Ya.Zverev, S.Yu. Makashov, V.V. Palchikovsky, A.F. Sobolev, V.V. Chernykh. Experimental study of sound absorption of acoustic wedges for an echo-free chamber// Acoustic journal. 2015. Vol. 61, No. 5.C. 636-644.

10. A.Ya. Zverev. Mechanisms of noise reduction in an aircraft cabin// Acoustic journal. 2016. Vol. 62, pages 474-479.
11. A.Ya. Zverev, B.M. Efimtzov. A comparative estimate of the acoustic emission of thin-walled structures excited by a turbulent boundary layer for various representations of the mutual spectrum, Acoustic journal. 2012. Volume 58, №4. Pages 459-464.
12. B.M. Efimtzov, L.A. Lazarev. A complex of analytical models for noise forecast in the aircraft cabin //Acoustic journal. 2012. Volume 58, №4. Pp. 443-449.
13. I.I. Bogolepov. Industrial soundproofing/Leningrad: Shipbuilding, 1986. 367 p.
14. N.I. Ivanov. Engineering acoustics. Theory and practice of noise control/Moscow: University Book, Logos, 2008. 424 p.
15. Experimental determination in acoustic chamber of sound-proof characteristics of GO / NTO panels, No. 5749, TsAGI, 2004.28 p.
16. Elaboration and justification of design measures to reduce acoustic loads acting on payload/NTO, No. 5088, TsAGI, 1993. 45 p.
17. A.G. Munin. Aircraft Acoustics. 2 parts. Part 2. Noise in passenger airliners/Moscow: Mechanical Engineering, 1986. 264 p.